genesis 40:231–240 (2004)

ARTICLE

Combined Haploid and Insertional Mutation Screen in the Zebrafish

Elizabeth Wiellette,[1] Yevgenya Grinblat,[1] Matthias Austen,[1] Estelle Hirsinger,[2] Adam Amsterdam,[3] Charline Walker,[2] Monte Westerfield,[2] and Hazel Sive[1,4]*

[1]Whitehead Institute for Biomedical Research, Cambridge, Massachusetts
[2]Institute of Neuroscience, University of Oregon, Eugene, Oregon
[3]Center for Cancer Research, Massachusetts Institute of Technology, Cambridge, Massachusetts
[4]Massachusetts Institute of Technology, Cambridge, Massachusetts

Received 30 September 2004; Accepted 2 October 2004

Summary: To identify genes required for development of the brain and somites, we performed a pilot screen of gynogenetic haploid zebrafish embryos produced from mothers mutagenized by viral insertion. We describe an efficient method to identify new mutations and the affected gene. In addition, we report the results of a small-scale screen that identified five genes required for brain development, including novel alleles of *nagie oko, pou5f1, ribosomal protein L36*, and *n-cadherin*, as well as a novel allele of the *laminin g1* gene that is required for normal skeletal muscle fiber organization and somite patterning. genesis 40:231–240, 2004.

Key words: zebrafish; haploid; insertional mutagenesis; brain; somite

INTRODUCTION

Genetic screens of chemically induced mutations in zebrafish have shown that the zebrafish is an excellent organism in which to identify and characterize the genes required for early vertebrate development. However, identification of the gene corresponding to a specific mutation frequently requires significant time and effort (Mullins, 2002). Insertional mutagenesis provides a faster way to identify the gene associated with a mutant phenotype, because the gene is "tagged" by the insertional agent. Currently, the most effective insertional mutagen in zebrafish is a pseudotyped retrovirus (Amsterdam, 2003). Infection with this virus is the basis for a highly successful screen for genes required for early embryonic development that has identified over 300 genes, or about 25% of the number of predicted genes required for embryonic development (Amsterdam, 2003; Amsterdam *et al.*, 1999, 2004a; Golling *et al.*, 2002).

For both chemical and insertional mutagenesis, identification of mutants has commonly relied on generation of F2 and F3 families, so that sibling matings can be used to produce homozygous diploids that reveal recessive mutant phenotypes (Driever *et al.*, 1996; Golling *et al.*, 2002; Haffter *et al.*, 1996). Because the generation time of zebrafish is 3–4 months, F2 family production can take almost a year from mutagenesis of the founders as embryos. However, zebrafish embryos survive as haploids for several days, and many aspects of haploid development are sufficiently normal that defects resulting from gene mutation can be identified (Patton and Zon, 2001; Walker, 1999). Mutagenesis screens of haploid embryos have been used for several years (Grunwald *et al.*, 1988), and have proven useful, leading to identification of genes including those required for development of the heart, notochord, and muscle (Alexander *et al.*, 1998; Halpern *et al.*, 1993; Moens *et al.*, 1996).

We have performed a pilot screen in which the techniques of insertional mutagenesis and haploid screening were combined. We screened for mutations that affect brain development, including brain morphogenesis and anteroposterior patterning of the early neural tube, and for mutations that affect somitogenesis. This method proved to be a rapid and effective way to screen inser-

Y. Grinblat and M. Austen contributed equally to this work.

Current address for Y. Grinblat: Departments of Zoology and Anatomy, University of Wisconsin, Madison, WI 53706.

Current address for M. Austen: DeveloGen AG, Goettingen 37079, Germany.

Current address for E. Hirsinger: Biologie moléculaire du Développement, Institut Pasteur, Paris 15 75724, France.

* Correspondence to: H. Sive, Massachusetts Institute of Technology, Cambridge, MA 02139.

E-mail: sive@wi.mit.edu

Contract grant sponsor: National Institutes of Health (NIH), Contract grant numbers: AR45575 and HD22486 (to M.W.); NIH HD08704 (to E.L.W.), Contract grant number: MH059942-04 (to H.L.S.), Contract grant sponsors: Charles King Trust (to Y.G.); Deutsche Forschungsgemeinschaft (to M.A.).

Published online in
Wiley InterScience (www.interscience.wiley.com)
DOI: 10.1002/gene.20090

tional mutant lines for defects in early developmental processes, and to identify the affected genes.

RESULTS

Pilot Haploid Insertional Screen

Adult founder females mutagenized by retroviral insertion (see Materials and Methods) were mosaic for random insertions of viral DNA throughout the genome, including the germline (Fig. 1). Eggs were expressed from the founder females and activated with irradiated sperm to induce development of gynogenetic haploid embryos (see Materials and Methods). These embryos were examined for abnormal haploid development, with specific attention to brain and somite formation.

Brain development was analyzed by fixing clutches of embryos at the tailbud stage (10 h postfertilization, hpf), followed by in situ hybridization with a cocktail of probes that highlighted the neural plate and regions of the presumptive fore-, mid-, and hindbrain domains (see Materials and Methods). In addition, morphology of the brain was analyzed at 30–32 hpf, at which time clutches of live embryos were examined for defects in brain morphology. Finally, at about 32 hpf, these clutches of embryos were fixed and analyzed for somite formation using antibodies directed against myosin heavy chain isoforms (see Materials and Methods).

To screen for brain and somite mutations, 327 clutches of embryos were examined for early brain patterning defects, 430 clutches for brain morphological defects, and 330 clutches for changes in myosin pattern in the somites. From Southern blot analysis of eggs isolated from founder females, we approximate that the germlines of the founder females contained an average of 12 insertions per female (data not shown). This indicates that about 3,924 insertions were screened for brain patterning defects, about 5,160 for brain morphology defects, and about 3,960 for somite defects.

Linkage of Phenotype With Viral Insertion and Cloning of Neighboring Genomic DNA

Because the germlines of founder females were mosaic, each insertion was present in the germline as a clone that differed in size between insertions. That is, clutches of embryos usually did not contain Mendelian ratios of mutant and wildtype embryos, but rather putative mutations were generally present in less than 50% of the embryos from a founder female. Specific phenotypes

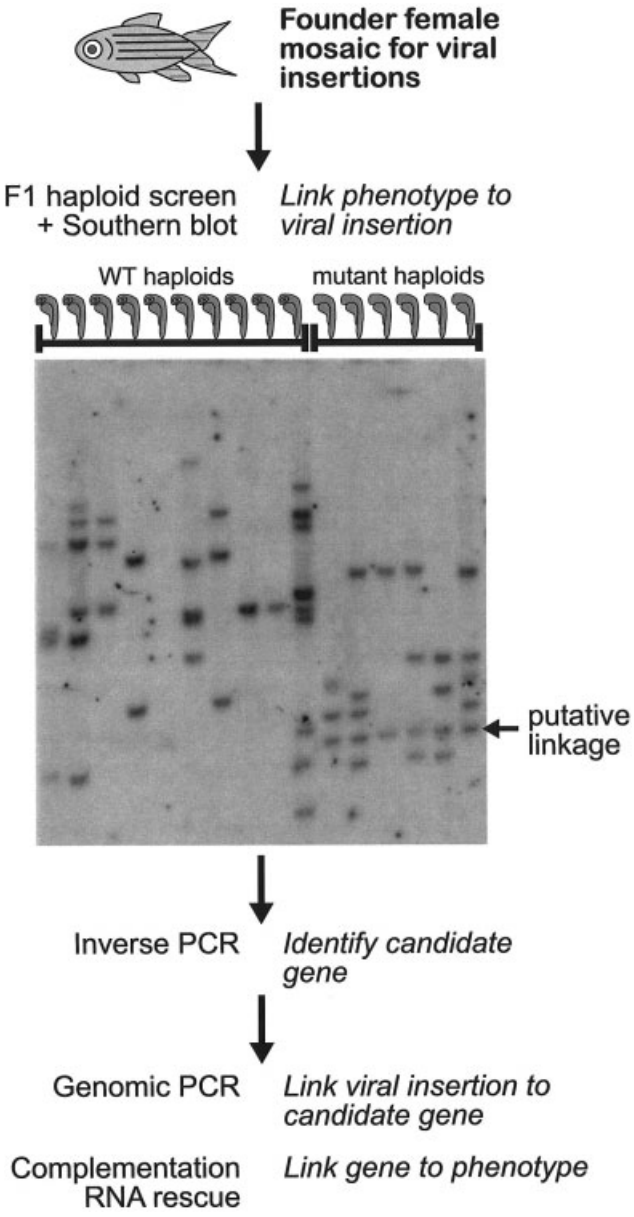

FIG. 1. Steps to identify mutations in haploid embryos and clone genes linked to insertions. Founder female fish were mutagenized by injection of retrovirus early in embryogenesis and independent insertions of the virus throughout the embryo resulted in adult fish that were mosaic in somatic and germline lineages (Amsterdam, 2003). Founder females were used to generate mosaic clutches of gynogenetic haploid embryos. If a mutant phenotype was observed in multiple embryos, these embryos were used directly to perform highly sensitive Southern blot analysis, with DNA from a single embryo analyzed in each lane. A representative Southern blot is shown, probed with viral sequence that hybridizes to bands including both viral and flanking genomic DNA (see Materials and Methods). Linkage of a mutant phenotype to a viral insertion is indicated by a common sized band present in all mutant embryos (arrow), and absent from all wildtype embryos. Genomic DNA flanking the viral insertion was cloned by inverse PCR. This primary genomic sequence sometimes included coding sequence for a gene, but other times this sequence was used to search genomic databases to identify genes predicted to be close to the primary sequence. PCR amplification of DNA between the candidate gene and the viral insertion was used to corroborate the physical linkage between a candidate gene and an insertion. Finally, confirmation that the phenotype results from changes in the candidate gene is gained from failure to complement an independent mutation in the candidate gene, or rescue of the phenotype by injection of the candidate gene mRNA.

Table 1
Summary of Linkages Between Viral Insertion, Phenotype, and Candidate Gene

Mutant line	Diploid phenotype	Candidate gene identity	Insertion linked to phenotype?[a]	Insertion linked to gene?[b]	Gene linked to phenotype?[c]
wi83	ventricles do not expand	*nagie oko* (*nok*)	Yes	Yes	Yes (*nagie oko*)
wi270	*pax2a,* r3 *egr2* (*krox20*) expression reduced defective MHB	*pou5f1*	Yes	Yes	Yes (*spiel-ohne-grenzen*)
wi371	midbrain ventricle does not form correctly, and 48 hr	*ribosomal protein L36*	Yes	Yes	Yes (*rpl36*)
	hindbrain ventricle swelling	*laminB2*		Yes	N/A
wi440	ventricles partially expand defective MHB	*cadherin 2, neuronal* (*cdh2*)	Yes	Yes	Yes (*parachute*)
wi513	severe necrosis throughout, starting in brain		Yes	No (tested RNA polII, lrg subunit)	N/A
wi390	short, wavy somite fibers short body axis	*laminin γ1*(*lamc1*)	Yes	Yes	Not tested

[a]"Insertion linked to phenotype" indicates that the insertion identified is tightly linked to the observed phenotype. Supporting data consist both of the initial Southern blot of genomic DNA from mutant and wildtype embryos and of at least three generations of continued linkage between the insertion and the phenotype, as assayed by the presence of the insertion in heterozygote carriers that give rise to 1/4 mutant progeny when mated.

[b]"Insertion linked to gene" indicates that there is a gene lying close to the insertion. Supporting data consist of PCR amplification between the viral sequence and the gene sequence in genomic DNA of the insertion line, resulting in a product of the expected size.

[c]"Gene linked to phenotype" indicates that a mutation in the candidate gene causes the observed phenotype. Supporting data consist of failure to complement in crosses between a carrier of the insertion and a known mutant allele of the candidate gene (listed in parentheses).

that appeared in more than 10% of the embryos in a clutch were further analyzed.

To determine whether a phenotype resulted from a specific viral insertion, embryos from a single clutch were sorted into those with mutant and wildtype phenotypes, and DNA was extracted from individual embryos for analysis. This DNA was digested, to release a fragment extending from a fixed point in the viral insertion to an unknown, unique position in the flanking genomic DNA, and analyzed by Southern blots probed with a viral sequence-directed probe. Blot sensitivity was optimized to allow detection of DNA from single embryos as described in Materials and Methods. Because the embryos were haploid, identification of a mutagenic insertion relied on a particular hybridizing band (comprising viral plus genomic DNA) being present in all mutant embryos and absent from all nonmutant embryos (Fig. 1).

After identifying a viral insertion that was linked to the phenotype of interest, we used inverse PCR methods to isolate genomic DNA surrounding the site of insertion. In many cases we were able to clone genomic DNA sequences by inverse PCR directly from the same genomic DNA samples prepared for the Southern blot, thereby saving the time required for reidentification of mutant embryos and preparation of new DNA samples. The probability that inverse PCR would amplify linked genomic sequence from a sample was dependent on the size of the fragment to be amplified, with fragments less than 4 kb more likely to be cloned. Comparison of DNA sequence surrounding the linked viral insertion with databases at the NCBI allowed us to identify a nearby candidate gene in all cases.

Corroboration of the Linkage Among Viral Insertion, Phenotype, and Candidate Gene

Initial linkage between a phenotype and a viral insertion was determined by correlating the presence of a particular insertion with the phenotype, and lack of the insertion in wildtype sibling embryos. Typically, our identification of the probable mutagenic insertion was based on analysis of at least 20 embryos. To confirm further that the phenotype was tightly linked to the insertion, we have shown that the phenotype and the insertion are still linked in the F3 generation of all lines (Table 1).

In the cases of *wi270* and *wi390*, the primary fragments of genomic DNA isolated by inverse PCR contained open reading frames for the genes *pou5f1* and *lamc1*, respectively. For the other four lines, the primary sequence was used to search genomic sequence assemblies for nearby genes that might be affected. PCR amplification of DNA between the candidate gene open reading frame and the viral sequence was performed to ensure that the insertion was situated at the predicted position relative to the candidate gene (Table 1). Only *wi513* failed to show physical linkage between the insertion and the predicted closest gene, *RNA polymerase II (large subunit)*. It is possible that the genomic sequence is misassembled in this region, or that the PCR failed for unrelated reasons, and therefore the data do not conclusively show whether *wi513* is located

close to *RNApolII*. The insertion *wi371* lies between two genes, *ribosomal protein L36 (rpl36)* and *lamin B2*, and might affect the expression or function of either or both genes. Finally, as described below, four of the six mutations identified have been confirmed to affect the nearby gene through complementation tests with independent mutant alleles of the gene (Table 1).

Mutations Affecting Brain Patterning and Morphology

Screening haploid embryos by in situ hybridization and by morphology both yielded mutations that produce brain defects. A single mutation that affects brain patterning at the tailbud stage, *wi270*, was identified by alterations in the RNA expression patterns of *pax2a* and *early growth response 2b (egr2b*; commonly known as *krox20*) as assayed by mRNA in situ hybridization. In addition, this mutation showed morphological defects in development of the midbrain/hindbrain boundary (MHB) and hindbrain (Fig. 2G–I). This insertion falls within the *pou5f1* open reading frame, and fails to complement $pou5f1^{bi349}$, an allele of *spiel ohne grenzen* (Table 1; Belting *et al.*, 2001; Burgess *et al.*, 2002), strongly suggesting that *wi270* affects the *pou5f1* gene. Gene expression patterns in the brain are similar between haploid and diploid embryos (Fig. 3A,C), and therefore screening for patterning defects in haploids is likely to be dependable. For example, in homozygous diploid *pou5f1* mutant embryos, *egr2b* and *pax2a* are expressed, but at severely reduced levels, and missing from the dorsal midline. In contrast, in haploid *pou5f1* mutants, *egr2b* and *pax2a* neural expression is missing entirely, although some *pax2a* expression remains in the otic placode (Fig. 3B,D).

Four mutations were identified as having defects that affect brain morphology. The *wi83* insertion lies within the first intron of the *nagie oko (nok*) gene (Wei and Malicki, 2002), and fails to complement aspects of the nok^{m226} phenotype, including failure of brain ventricles to expand and axial curvature (Figs. 2D–F, 4A–C). However, nok^{m226} homozygous mutants additionally exhibit retinal disorganization (Wei and Malicki, 2002), evidenced by reduction or loss of pigmentation (Fig. 4C), whereas nok^{wi83} homozygous embryos exhibit normal eye pigmentation, suggesting that nok^{wi83} is a hypomorphic allele. Haploid *wi83* mutants have defects in the forebrain (Fig. 2F) similar to the foreshortened appearance of *nok* diploid mutant embryos at 48 hpf (Fig. 4).

The insertion, *wi440*, lies within an intron of the *neuronal cadherin 2 (cdh2*) gene, and fails to complement $ncad^{tm101}$, a mutation in *cdh2* (Lele *et al.*, 2002), as well as *hi1389*, an independent viral insertion within the *cdh2* gene (Amsterdam *et al.*, 2004a). As reported for other *ncad* alleles, the MHB fails to form correctly, and the hindbrain ventricle develops irregular edges (Fig. 2M–O; Jiang *et al.*, 1996; Lele *et al.*, 2002). Although the defect in homozygous *wi440* diploid embryos is strongest in the hindbrain, the mutation also causes obvious defects in the eyes and forebrain in the haploids (Fig. 2O).

The insertion, *wi371*, lies between two putative gene sequences in the zebrafish genome, *ribosomal protein L36 (rpl36*) and *lamin B2* (Table 1). This mutation fails to complement another insertional allele that has been shown to cause a defect in $rpl36^{hi1807}$ (Amsterdam *et al.*, 2004b). The *wi371* mutant phenotype looks similar to inflated hindbrain ventricle phenotypes produced by other insertions lying close to or within ribosomal protein genes (Fig. 2J–L) (Amsterdam *et al.*, 2004b; Golling *et al.*, 2002). Again, it is interesting that a defect that appears to affect mainly the hindbrain ventricle in homozygous diploid mutants has a stronger effect on the midbrain in haploid mutants (Fig. 2L).

Although the *wi513* insertion appears to be close to the predicted gene encoding the RNA polymerase II large subunit, an attempt to link the gene to the insertion by PCR of genomic DNA did not support the expected proximity between the two sequences. Therefore, it is not clear which gene(s) may be affected by the *wi513* insertion. The defects observed in *wi513* homozygous diploid and haploid embryos include severe degeneration of tissues, particularly in the head (Fig. 2P–R).

Additionally, in the screens for brain defects we identified four founders carrying mutations of interest that were present in the germline, but that were not linked to a viral insertion. In addition to nonlinkage to an insertion, one of these mutations did not transmit to the next generation, suggesting that it may have been a dominant mutation. The other three mutations have been propagated into subsequent generations. Finally, four founders carrying linked mutagenic insertions of interest were identified, but the founder fish were lost without establishing lines of fish carrying the mutations.

Genes Required for Somite Development

Two mutations that affect somite development were identified and the gene affected in one of these was successfully cloned. Homozygous diploid embryos mutant for the *wi390* viral insertion have a shortened body axis. The normal number of somites form, but they are shorter along the anteroposterior axis and taller along the dorsoventral axis (Fig. 5). As evidenced by the presence of S58 slow myosin and MF20 pan-muscle labeling, both slow and fast muscle fibers form in *wi390* mutants. Muscle fibers are striated and span the length of the somite. However, both slow and fast muscle fibers are abnormally organized, appearing short and wavy (Fig. 5). The horizontal myoseptum is missing. The *wi390* viral insertion lies within the first exon of the *laminin γ1 (lamc1*) gene, and the defects observed match those previously described for *lamc1* mutants, including a shortened body axis (Parsons *et al.*, 2002). Therefore, it is highly likely that *wi390* is a defect in the *lamc1* gene. Two additional founder females carried reproducible somite mutations for which we could not find a linked insertion.

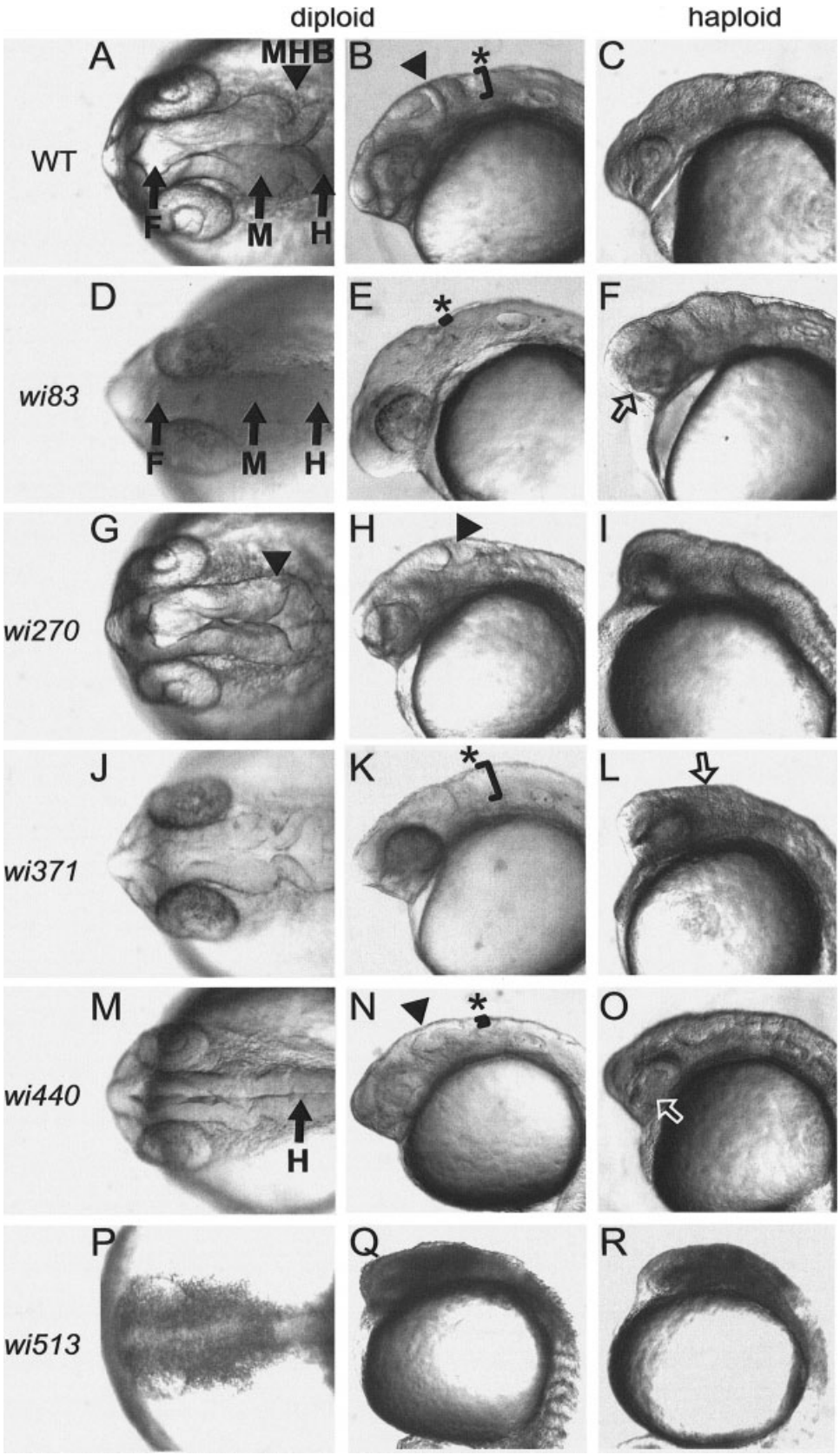

FIG. 2. Phenotypes of mutations affecting brain development. All embryos are ~24 hpf. (**A,D,G, J,M,P**) dorsal views, (**B,C,E,F, H,I,K,L,N,O,Q,R**) lateral views. (**C,F,I,L,O,R**) haploid embryos. **A–C:** wildtype embryos: arrows indicate forebrain (F), midbrain (M), and hindbrain (H) ventricles, arrowhead indicates the midbrain/hindbrain boundary (MHB). Bracket and asterisk indicate the depth of the hindbrain ventricle (**B**). Haploid embryos (**C**) do not develop a well-defined MHB, nor well-formed ventricles. **D–F:** *wi83*, in which the brain ventricles do not form (arrows, **D**; asterisk highlights severely reduced bracket, **E**). *wi83* haploid embryos were initially identified based on their mildly cyclopic phenotype (open arrow, **F**). **G–I:** *wi270*, in which the MHB does not form correctly (arrowhead). **J–L:** *wi371*, in which the hindbrain ventricle overexpands (bracket and asterisk, **K**), and the haploid mutants were initially identified by necrosis specific to the midbrain (open arrow, **L**). **M–O:** *wi440*, in which the hindbrain ventricle only partially expands (arrow, **M**; asterisk indicates severely reduced bracket, **N**), and the MHB is not well formed (arrowhead, **N**). The haploid phenotype was initially identified as small eyes and forebrain (open arrow, **O**). **P–R:** the *wi513* phenotype consists of brain-specific necrosis in both homozygous diploids (**P,Q**) and haploids (**R**).

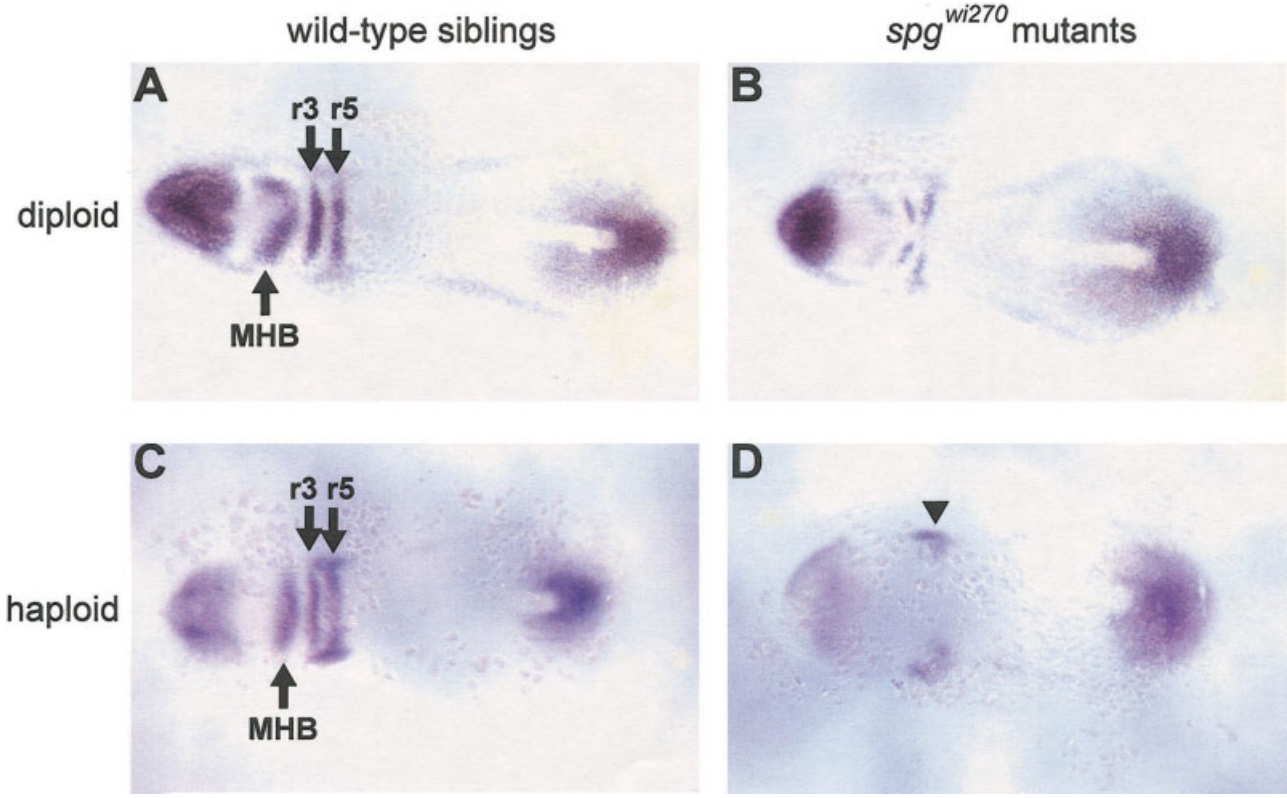

FIG. 3. Comparison of *spg*^{wi270} phenotypes in diploid and haploid embryos. **A–D:** Embryos in situ hybridized with *dlx3b, rx3, pax2, egr2b, tbx6* at 12 hpf. **A,B:** Diploid embryos showing wildtype (**A**) and mutant (**B**) labeling patterns. In these mutants, expression of *pax2a* (MHB) and *egr2b* (r3, r5) is reduced, particularly at the midline. **C,D:** Haploid embryos showing wildtype (**C**) and mutant (**D**) labeling pattern. Staining is similar between haploid and diploid embryos, although in haploid mutants the loss of *pax2a* and *egr2b* expression is more severe than in the homozygous diploid embryos, with the only *pax2a* in the otic placode and potentially some *egr2b* in r5 remaining (arrowhead, **D**). Arrows highlight expression of genes in the forming midbrain/hindbrain boundary (MHB) and rhombomeres 3 and 5 (r3, r5).

DISCUSSION

Advantages and Disadvantages of Haploid Insertional Screening

This pilot screen combined the benefits of insertional mutagenesis that include rapid identification of putative mutated genes with the advantages of haploid genetics that allows screening F0 or F1 fish, decreasing the time between mutagenesis and screening. We chose to screen embryos generated from founder (F0) fish, rather than from F1 fish, an approach that saved breeding time and tank space. A drawback to our approach was that by working directly with founder females, we risked losing a line of interest if the female did not survive the squeezing process used to generate haploids, or if she did not produce another clutch of eggs by squeeze or normal mating. This problem could be overcome by mating individual females prior to the gynogenesis and raising the offspring to maintain the line (Alexander *et al.*, 1998).

Haploid screening of insertional mutations directly from the founder reduced the possibility of identifying a spontaneous mutation tightly linked to a nonmutagenic insertion. The expected ratio of embryos mutated by viral insertion was less than 50%, whereas background mutations accumulated in the genome would appear at a rate of 50%, and thus could be selected against. Spontaneous mutations arising during development of the F0 germline were unlikely to occur at the same rate and in the same distribution as a viral insertion, and therefore would appear unlinked to the viral insertion.

We isolated four lines exhibiting mutations that segregated with mendelian frequency but were not linked to a viral insertion according to Southern analysis. Because these mutations were present in the screened clutches at a frequency significantly different from 50%, we suspect that the mutations arose during development of the founders. While we have not examined the molecular nature of these mutations, we speculate that they may be caused by insertion of viral sequence fragments, excluding the sequence from which the Southern probe was made. It is unlikely that these mutations are caused by viral insertion followed by imprecise excision or chromosomal rearrangement, since the retrovirus used for this mutagenesis is replication-defective and therefore expected to remain stably integrated in the genome (Amsterdam and Hopkins, 1999). At a frequency similar to our results,

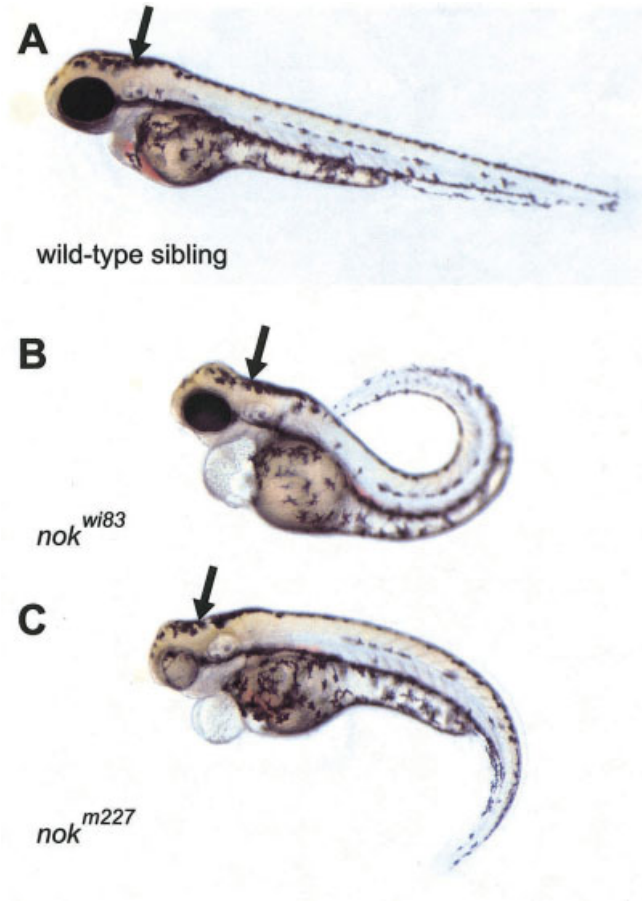

FIG. 4 Comparison of *nagie oko* mutant allele phenotypes. Live embryos are shown at ~48 hpf. **A:** Wildtype embryo showing normal morphology, including normal expansion of the hindbrain ventricle (arrow). **B:** The hypomorphic allele *nok*^{wi83} isolated in this screen. The hindbrain ventricle fails to develop correctly, which is apparent in the concave appearance of the mutant embryo hindbrain (arrow). Also, after initially normal development, the tail "flips" and stays curved. **C:** The null allele *nok*^{m227} also develops a sunken hindbrain (arrow), and the tail curves after initial normal development. In addition, the eye almost entirely lacks pigment probably due to a lack of epithelial polarity (Jensen and Westerfield, 2004; Wei and Malicki, 2002). [Color figure can be viewed in the online issue, which is available at www.interscience.wiley.com.]

approximately one-quarter of the mutations recovered in the F_3 screen were not linked to detectable insertions, and these were attributed to spontaneous mutations (Amsterdam, 2003). However, the rate of spontaneous mutations generated in a single generation should be lower than that observed after three generations. Thus, it is possible that at least some of our nonlinked mutations result from an unexpected consequence of viral infection, probably insertion of a viral sequence fragment.

Identification of Brain Development Mutations in Haploids

In haploid embryos, the brain fails to develop many common landmarks, including the MHB and ventricles (Fig. 2C). A significant number (3/4) of the mutations that we identified on the basis of morphological defects in the brain appeared to have different phenotypes in haploids and homozygous diploids. For example, the *wi440* mutation, an allele of *ncad*, was identified in haploid embryos based on small eyes and forebrain, but is characterized in homozygous diploids as having defects in the tectum and hindbrain ventricle. However, of all the mutant lines isolated from screening haploids, none failed to show an interesting diploid mutant phenotype. In addition, gene expression patterns at early stages are very similar between haploid and diploid embryos. Therefore, the analysis of mutant phenotypes in haploid embryos is a useful way to identify mutations that affect brain development.

Identification of a Novel Allele of *nok*

One of the mutations isolated, *wi83*, is a hypomorphic allele of *nok*. The insertion that created the mutant phenotype lies within the first intron of the gene. The *nok* allele identified in our screen displays defects in brain ventricle expansion and a curved body axis, but does not develop the eye pigment disorganization that is observed in other *nok* allele mutants (Wei and Malicki, 2002). It is possible that *wi83* has reduced levels of the *nok* transcript, and that only the brain ventricles and axial curvature are sensitive to this reduction, while the eye is not. Preliminary α-NOK data show that some NOK protein remains in *wi83* mutants (L.A. Lowery and H. Sive, unpubl. data), suggesting that the viral insertion reduces the amount or length of *nok* transcripts, but does not entirely abolish NOK protein production in this mutant background. The NOK protein translation start falls after the first intron, and therefore beyond the viral insertion within the first intron. It is most likely that the insertion causes a reduction in the level of *nok* expression, since these viral insertions commonly cause reduced levels of expression (Amsterdam, 2003).

Identification of a New Allele Reveals a Role of Laminin in Somite Development

Analysis of the *lamc1* mutation, *sleepy*, revealed a role for *laminin* in notochord development (Parsons *et al.*, 2002). We previously showed that *laminin* is distributed throughout the central region of the somites during the early phase of motor axon outgrowth (Westerfield, 1987). It is also expressed at somite boundaries (Parsons *et al.*, 2002). However, the function of *laminin* in the somites had not been described previously. Our analysis of the new allele of *lamc1, wi390*, obtained in our insertional mutation screen, demonstrates that *laminin* is required for proper organization of skeletal muscle fibers in the somites. On the other hand, somite segmentation and myogenesis are relatively normal in *lamc1* mutants, suggesting that *laminin* plays little or no role in these processes. Because horizontal myoseptum formation requires signals from the notochord, the absence of the horizontal

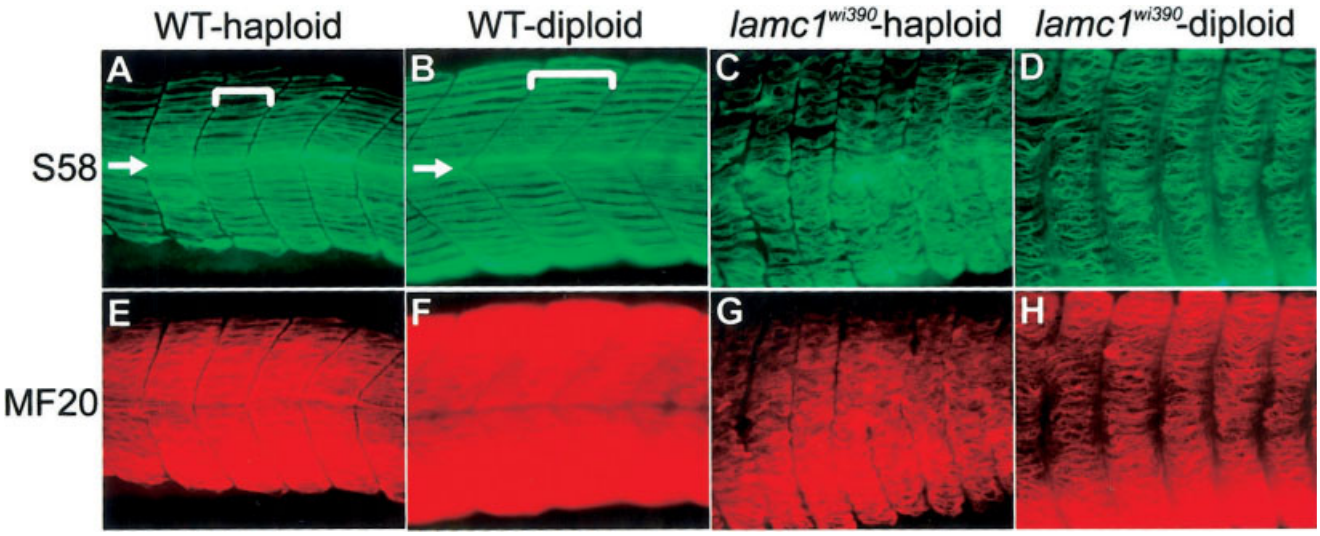

FIG. 5. Function of *lamc1* gene in skeletal muscle patterning. Embryos were analyzed at 32 hpf. **A–D:** The S58 antibody labels slow muscle-specific myosin heavy chain and zebrafish slow muscle fibers (Devoto *et al.*, 1996). In wildtype haploid (**A**) and diploid (**B**) embryos, slow muscle fibers are straight and consistently spaced (individual somites indicated with brackets), whereas in mutant haploid (**C**) and homozygous diploid (**D**) embryos, the somites are shorter and the slow muscle fibers are wavy and somewhat disorganized. **E–H:** The MF20 antibody recognizes myosin heavy chain in both slow and fast zebrafish skeletal muscle fibers and reveals a phenotype identical to S58. Wildtype haploid (**E**) and homozygous diploid (**F**) embryos form straight muscle fibers, whereas mutant haploid (**G**) and homozygous diploid (**H**) embryos develop wavy, disorganized fibers. White arrows indicate the horizontal myoseptum in S58-labeled wildtype haploid and diploid embryos.

myoseptum is most likely due to the defects in notochord formation (Parsons *et al.*, 2002). Notochord defects can affect the length of the axis, although the wavy and disorganized patterning of muscle fibers and shortened somites could also account for the truncated body length in *lamc1* mutants.

Conclusion

We have demonstrated that a coupled haploid and insertional mutation screen is feasible and efficient. We suggest that this method is a useful addition to the repertoire of zebrafish genetic screening tools.

MATERIALS AND METHODS

Mutagenesis and Husbandry

Embryos were mutagenized by injection of retrovirus at about the 1,000-cell stage, then raised to adulthood (Amsterdam *et al.*, 1999). Fish lines were raised and maintained according to general practices as described in Westerfield (2000).

Haploid Embryo Production

Founder females were mated to males 10 days before haploid production and productive females were maintained in small groups isolated from males until haploid production. The night before haploid production, females were set up in batches with males separated by a screen to prevent natural mating. Males thus "pseudomated" were squeezed to obtain sperm, as described (Walker, 1999; Westerfield, 2000). Sperm from about 60 males was collected into no less than 500 μL of Hank's solution and UV-irradiated at 120 mJ (UV Stratalinker 1800, Stratagene, La Jolla, CA). Females were squeezed to obtain eggs as described (Walker, 1999; Westerfield, 2000). About 15 μL of irradiated sperm was added to each clutch of healthy eggs and the eggs were activated and allowed to grow in Embryo Medium (Westerfield, 2000). Each female was given a specific number and maintained in isolation while embryo analysis was performed.

Large clutches (more than 75 embryos) of healthy haploid embryos were divided into two groups, one of which was fixed at the one somite stage for in situ hybridization analysis of gene expression in the presumptive brain, and the other was raised to 32 hpf for analysis of somite development using antibody markers. Smaller clutches were not split and were designated for one screen or the other. The female was then reused later to generate a clutch for screening by the alternate method.

Visual Screen for Morphological Defects

Embryos were examined for morphological defects at 30–32 hpf, with particular emphasis on the brain. Although haploid embryos have extensive defects, particularly in the brain (Fig. 2C), we were able to identify defects beyond those common in haploid embryos (Fig. 2) (Patton and Zon, 2001; Walker, 1999).

mRNA In Situ Hybridization Screen for Brain Pattern Defects

Embryos were fixed and labeled by mRNA in situ hybridization with a cocktail of probes following previously described methods (Sagerstrom *et al.*, 1996). Probes used were *sonic hedgehog (shh*; expressed in axial mesoderm; Krauss *et al.*, 1993), *tbx6* (expressed in the tailbud; Hug *et al.*, 1997), *egr2b (krox20*) (expressed in rhombomeres 3 and 5; Oxtoby and Jowett, 1993), *dlx3b* (expressed in placodal ectoderm adjacent to the margin of the neural plate; Akimenko *et al.*, 1994), *pax2a* (midbrain/hindbrain boundary; Krauss *et al.*, 1991), and *rx3* (expressed in the anterior neural plate; Loosli *et al.*, 2003). Expression patterns of these genes are very similar in haploid and diploid embryos during early somitogenesis. Clutches of embryos were examined for missing or disrupted gene expression.

Antibody Screen for Somite Defects

Embryos were prepared essentially as described previously (Alexander et al., 1998) and were hybridized with the monoclonal antibodies MF20 that recognizes myosin heavy chain (Bader *et al.*, 1982), and S58 that recognizes myosin heavy chain isoforms specific to slow muscle fibers (Miller *et al.*, 1985). Secondary antibodies used were anti-IgG2b-TRITC that binds MF20, and anti-IgA-FITC that binds S58 (Southern Biotechnology Associates, Birmingham, AL).

Southern Blot to Identify Linked Insertions

High-sensitivity Southern blots were performed to identify viral insertions present in each haploid embryo. Genomic DNA was digested with BglII, which created a uniquely sized fragment for each viral insertion extending from the single viral BglII site to the next BglII site within the genomic sequence. Viral insertions were identified on the Southern blot using a probe directed against 1 Kb of viral sequence included in the BglII digest.

Individual embryos identified as mutants by morphology, antibody labeling, or in situ hybridization, and some siblings for reference, were put into separate 1.5 mL tubes and incubated at 55°C overnight in 50 μL ELVIS buffer (Amsterdam *et al.*, 1999) + 1 μL 10 mg/mL proteinase K. Each sample was then extracted twice with 50:49:1 phenol:chloroform:isoamyl alcohol, and once with chloroform. DNA was precipitated in 1 μL 20 mg/mL glycogen, 17 μL 10 M ammonium acetate, and 100 μL ethanol at −20°C for 1 h, and centrifuged at 4°C for 20 min. The entire DNA sample was resuspended in 2.5 μL NEB Buffer 3, 2.5 μL spermidine, 2 μL BglII, 18 μL H_2O, and the digests were incubated at 37°C overnight. Twenty μL (80%) of each digested sample was then loaded on a 0.8% agarose gel with 1× TAE buffer and run at 200V for about 3 h. The gel was denatured in 0.4 M NaOH for 20–30 min, then transferred to GeneScreen Plus membrane (NEN Life Science, Boston, MA) using 0.4 M NaOH for the transfer buffer. After transfer was complete (2.5 h to overnight), the membrane was rinsed in 2× SSC and crosslinked while still damp at 2,400 × 100 mJ/cm^2 in a UV Stratalinker 1800 (Stratagene).

High specific activity probe was made by unidirectional PCR. The PCR reaction consisted of: 2 μL (0.1 mg/mL) template fragment, 1 μL 20 mM primer (directed against one end of the template sequence), 2 mL H_2O, 1.5 mL 10× PCR buffer, 7.5 μL α-^{32}P-dCTP (3,000 Ci/mmol; 13.3 μM), 0.5 μL dNTP mix (0.5 mM dATP, dGTP, dTTP, 0.3 mM dCTP), 0.5 μL HotStarTaq (Qiagen, Valencia, CA). Forty cycles were run at: 94°C, 45 sec, 60°C 45 sec, 72°C 1 min. Free nucleotides were removed by running the reaction over a G50 spin column.

The blot was prehybridized in Church buffer (7% SDS, 0.125 M sodium phosphate pH 7.4, 1% BSA, 5 mM EDTA, 0.1 mg/mL sonicated salmon sperm DNA), and hybridized overnight at 65°C with 1 mL Church buffer / 10 cm^2 blot and the entire probe sample. Washes consisted of two short rinses at room temperature in 0.2× SSC + 0.1% SDS, followed by 2-3 washes at 65°C with 0.1× SSC + 0.1% SDS over 2–3 h. BioMaxMS (Kodak) film was used in combination with a BioMax enhancer screen (Kodak).

Inverse PCR to Clone Genomic Fragments

To clone genomic DNA flanking a viral insertion of interest, a portion of BglII-digested DNA reserved from the Southern blot was used. It is difficult to clone large (>4 kb) fragments by this method. Therefore, if the insertion of interest produced a large (>4 kb) fragment, new DNA samples were digested with TaqαI that also targets a unique site within the viral sequence, and reanalyzed by Southern blot in the hope of finding a more appropriate sample on which to perform inverse PCR. Ligations were set up as follows: 1 μL BglII/TaqαI digest, 5.5 μL 10× ligation buffer, 0.5 μL T4 DNA ligase, 48 μL H_2O, incubated at 16°C overnight. Ligated samples were precipitated with: 1 μL glycogen, 18 μL (10M) ammonium acetate, 110 μL ice-cold ethanol. The pellet was resuspended directly in the 50 μL PCR reaction mix (5 μL buffer, 0.5 μL (10 mM) dNTPs, 1 μL (20 μM) each primer, 0.5 μL Taq polymerase, 42 μL H_2O). Alternatively, larger (2–4 kb) fragments were amplified using 0.5 μL Pfu turbo polymerase (Stratagene) and a longer (9 min) extension time. Primers were directed against the 5′ end of the viral sequence and the region just within the BglII site, oriented away from the central virus sequence. PCR products were gel purified, using the QIAquick Gel Extraction Kit (Qiagen), reprecipitated with glycogen as above, and resuspended in the pGEM-T Easy Vector Ligation reaction (Promega, Madison, WI). This reaction was used to transform chemically competent cells (DH5α; Invitrogen, Carlsbad, CA) using recommended methods and plasmids purified from transformed cells were used for sequencing.

ACKNOWLEDGMENTS

We thank Rachael Daly for expert technical help, and Ben Pratt, Amy Tatum, and Brian Kelly. We also thank

Shawn Burgess, Wenbiao Chen, Greg Golling, and Maryann Haldi for production of the injected virus and founder fish. We thank Laura Anne Lowery for communication of her unpublished results.

LITERATURE CITED

Akimenko MA, Ekker M, Wegner J, Lin W, Westerfield M. 1994. Combinatorial expression of three zebrafish genes related to distal-less: part of a homeobox gene code for the head. J Neurosci 14:3475–3486.

Alexander J, Stainier DY, Yelon D. 1998. Screening mosaic F1 females for mutations affecting zebrafish heart induction and patterning. Dev Genet 22:288–299.

Amsterdam A. 2003. Insertional mutagenesis in zebrafish. Dev Dyn 228:523–534.

Amsterdam A, Hopkins N. 1999. Retrovirus-mediated insertional mutagenesis in zebrafish. Methods Cell Biol 60:87–98.

Amsterdam A, Burgess S, Golling G, Chen W, Sun Z, Townsend K, Farrington S, Haldi M, Hopkins N. 1999. A large-scale insertional mutagenesis screen in zebrafish. Genes Dev 13:2713–2724.

Amsterdam A, Nissen RM, Sun Z, Swindell EC, Farrington S, Hopkins N. 2004a. 315 Genes essential for early zebrafish development. Proc Natl Acad Sci USA 101:12792–12797.

Amsterdam A, Sadler KC, Lai K, Farrington S, Bronson RT, Lees JA, Hopkins N. 2004b. Many ribosomal protein genes are cancer genes in zebrafish. PLoS Biol 2:E139.

Bader D, Masaki T, Fischman DA. 1982. Immunochemical analysis of myosin heavy chain during avian myogenesis in vivo and in vitro. J Cell Biol 95:763–770.

Belting HG, Hauptmann G, Meyer D, Abdelilah-Seyfried S, Chitnis A, Eschbach C, Soll I, Thisse C, Thisse B, Artinger KB, Lunde K, Driever W. 2001. Spiel ohne grenzen/pou2 is required during establishment of the zebrafish midbrain-hindbrain boundary organizer. Development 128:4165–4176.

Burgess S, Reim G, Chen W, Hopkins N, Brand M. 2002. The zebrafish spiel-ohne-grenzen (spg) gene encodes the POU domain protein Pou2 related to mammalian Oct4 and is essential for formation of the midbrain and hindbrain, and for pre-gastrula morphogenesis. Development 129:905–916.

Devoto SH, Melancon E, Eisen JS, Westerfield M. 1996. Identification of separate slow and fast muscle precursor cells in vivo, prior to somite formation. Development 122:3371–3380.

Driever W, Solnica-Krezel L, Schier AF, Neuhauss SC, Malicki J, Stemple DL, Stainier DY, Zwartkruis F, Abdelilah S, Rangini Z, Belak J, Boggs C. 1996. A genetic screen for mutations affecting embryogenesis in zebrafish. Development 123:37–46.

Golling G, Amsterdam A, Sun Z, Antonelli M, Maldonado E, Chen W, Burgess S, Haldi M, Artzt K, Farrington S, Lin SY, Nissen RM, Hopkins N. 2002. Insertional mutagenesis in zebrafish rapidly identifies genes essential for early vertebrate development. Nat Genet 31:135–140.

Grunwald DJ, Kimmel CB, Westerfield M, Walker C, Streisinger G. 1988. A neural degeneration mutation that spares primary neurons in the zebrafish. Dev Biol 126:115–128.

Haffter P, Granato M, Brand M, Mullins MC, Hammerschmidt M, Kane DA, Odenthal J, van Eeden FJ, Jiang YJ, Heisenberg CP, Kelsh RN, Furutani-Seiki M, Vogelsang E, Beuchle D, Schach U, Fabian C, Nusslein-Volhard C. 1996. The identification of genes with unique and essential functions in the development of the zebrafish, Danio rerio. Development 123:1–36.

Halpern ME, Ho RK, Walker C, Kimmel CB. 1993. Induction of muscle pioneers and floor plate is distinguished by the zebrafish no tail mutation. Cell 75:99–111.

Hug B, Walter V, Grunwald DJ. 1997. tbx6, a Brachyury-related gene expressed by ventral mesendodermal precursors in the zebrafish embryo. Dev Biol 183:61–73.

Jensen AM, Westerfield M. 2004. Zebrafish mosaic eyes is a novel FERM protein required for retinal lamination and retinal pigmented epithelial tight junction formation. Curr Biol 14:711–717.

Jiang YJ, Brand M, Heisenberg CP, Beuchle D, Furutani-Seiki M, Kelsh RN, Warga RM, Granato M, Haffter P, Hammerschmidt M, Kane DA, Mullins MC, Odenthal J, van Eeden FJ, Nusslein-Volhard C. 1996. Mutations affecting neurogenesis and brain morphology in the zebrafish, Danio rerio. Development 123:205–216.

Krauss S, Johansen T, Korzh V, Fjose A. 1991. Expression of the zebrafish paired box gene pax[zf-b] during early neurogenesis. Development 113:1193–1206.

Krauss S, Concordet JP, Ingham PW. 1993. A functionally conserved homolog of the Drosophila segment polarity gene hh is expressed in tissues with polarizing activity in zebrafish embryos. Cell 75:1431–1444.

Lele Z, Folchert A, Concha M, Rauch GJ, Geisler R, Rosa F, Wilson SW, Hammerschmidt M, Bally-Cuif L. 2002. Parachute/n-cadherin is required for morphogenesis and maintained integrity of the zebrafish neural tube. Development 129:3281–3294.

Loosli F, Staub W, Finger-Baier KC, Ober EA, Verkade H, Wittbrodt J, Baier H. 2003. Loss of eyes in zebrafish caused by mutation of chokh/rx3. EMBO Rep 4:894–899.

Miller JB, Crow MT, Stockdale FE. 1985. Slow and fast myosin heavy chain content defines three types of myotubes in early muscle cell cultures. J Cell Biol 101:1643–1650.

Moens CB, Yan YL, Appel B, Force AG, Kimmel CB. 1996. Valentino: a zebrafish gene required for normal hindbrain segmentation. Development 122:3981–3990.

Mullins MC. 2002. Building-blocks of embryogenesis. Nat Genet 31:125–126.

Oxtoby E, Jowett T. 1993. Cloning of the zebrafish krox-20 gene (krx-20) and its expression during hindbrain development. Nucleic Acids Res 21:1087–1095.

Parsons MJ, Pollard SM, Saude L, Feldman B, Coutinho P, Hirst EM, Stemple DL. 2002. Zebrafish mutants identify an essential role for laminins in notochord formation. Development 129:3137–3146.

Patton EE, Zon LI. 2001. The art and design of genetic screens: zebrafish. Nat Rev Genet 2:956–966.

Sagerstrom CG, Grinbalt Y, Sive H. 1996. Anteroposterior patterning in the zebrafish, Danio rerio: an explant assay reveals inductive and suppressive cell interactions. Development 122:1873–1883.

Walker C. 1999. Haploid screens and gamma-ray mutagenesis. In: Detrich W, Westerfield M, Zon LI, editors. The zebrafish: genetics and genomics. San Diego: Academic Press. p 44–70.

Wei X, Malicki J. 2002. Nagie oko, encoding a MAGUK-family protein, is essential for cellular patterning of the retina. Nat Genet 31:150–157.

Westerfield M. 1987. Substrate interactions affecting motor growth cone guidance during development and regeneration. J Exp Biol 132:161–175.

Westerfield M. 2000. The zebrafish book, 3rd ed. Eugene: University of Oregon Press.